Paper No. 455. (quote when citing this article)
Eleventh World Conference on Earthquake Engineering
ISBN: 0 08 042822 3

THREE DIMENSIONAL FAILURE OF RC COLUMNS IN BIAXIAL SHEAR

T. ICHINOSE

Department of Architecture, Nagoya Institute of Technology,
Gokiso, Showa, Nagoya 466, Japan

ABSTRACT

Antisymmetric bending shear was imposed on four specimens. Test parameters were shear reinforcement ratios (p_w = 0.75% and 1.18%) and loading directions (0 and 45 degrees). At their maximum deflections, fluorescent epoxy resin was injected into the specimens. After the tests, the specimens were sawed in transverse directions. Most of the cracks at the sections were curved, which means that shear failure was three dimensional.

Analyses were performed assuming rigid-plasticity of steel and concrete, utilizing the upper bound theorem of plasticity. Shear failure was assumed to occur three-dimensionally, sliding at curved cracks connecting the corners of shear reinforcement. The analyses explained the observed shear strength and failure pattern. The analysis also explained the effects of sub-ties on shear strength and failure pattern.

KEYWORDS

beam; columns; crack; detailing; plasticity; reinforced concrete; shear reinforcement; shear strength; shear failure; upper bound theorem.

BACKGROUND AND OBJECT

Shear failure is still an important factor in considering seismic resistance of reinforced concrete (RC) columns as demonstrated in 1995 Hyogoken-Nambu Earthquake in Japan. As Schlaich *et al.* [1987] pointed out, shear resistant mechanism in RC columns called truss action may include three dimensional conversion of inclined compressive stress of concrete into transverse tensile stress of individual hoop reinforcement as shown in Fig. 1(a)-(d). Stress field in a section subjected to shear force in 45 degree may be like Fig. 1(e). These figures imply that the effective depth of the truss action may be affected by the existence of sub-ties and the spacing of shear reinforcement. In fact, the experiments by Ichinose *et al* (1995) showed that these factors affected shear strength as much as 25%. If shear resistant mechanism is three dimensional, shear failure may be also three dimensional, which is exemplified in this paper.

EXPERIMENT

The loading and measuring apparatus is shown in Fig. 2. The two jacks were controlled to achieve antisymmetric deformation in the central part, which was 400 mm long. Rotation angles of the two stubs of the specimens were monitored by the two displacement transducers.

Tested were four specimens. They had an identical section shown in Fig. 3(a), where S6 and S8 indicate spirally grooved bars with diameters of 6 and 8 mm, and D22 and D13 indicate normal deformed bars with diameters of 22 and 13 mm. The specimens' names are L-0, H-0, L-45, and H-45: the first portion of the names, L or H, indicates that the diameter of the shear reinforcement is small or large (6 or 8 mm); the second portion, 0 or 45, indicates that the loading direction is 0 or 45 degree. Since the compressive stress of the truss action can exist inside the region enclosed by the outer tie as shown in Fig. 1, shear reinforcement ratio p_{we} is defined as follows:

$$p_{we} = \frac{a_w}{b_e \cdot s} \tag{1}$$

where b_e is the sectional area of shear reinforcement, b_e is the width of the section confined by the outer tie (in this case, b_e = 210 mm), and s is the spacing of shear reinforcement. According this definition, p_{we} of L or H specimens are 0.75% or 1.18%, respectively.

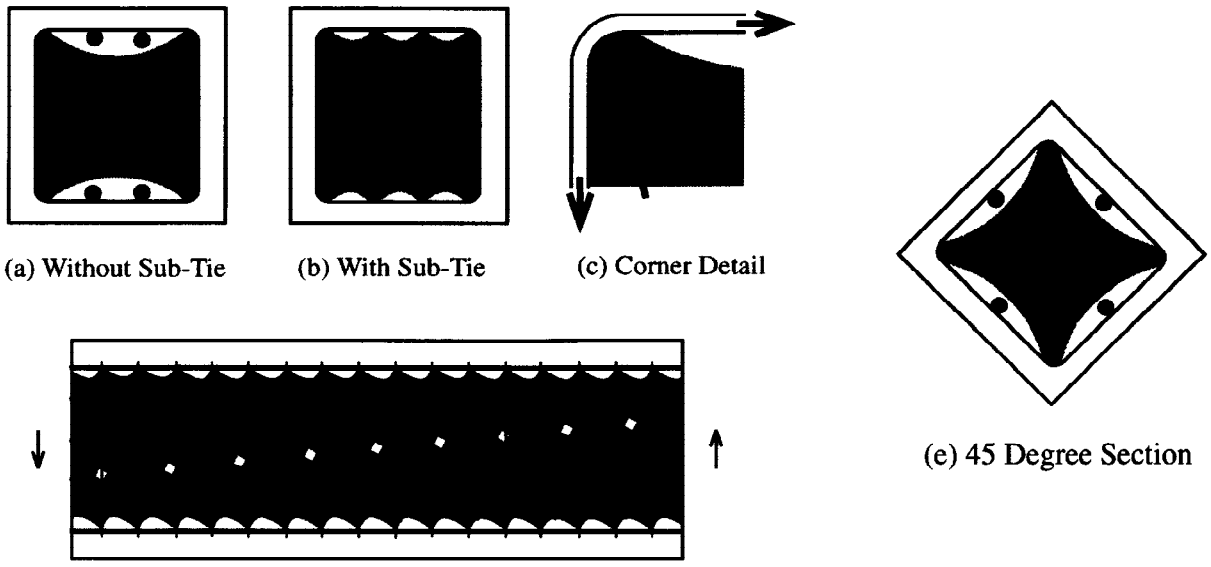

Fig. 1 Compressive stress field in section

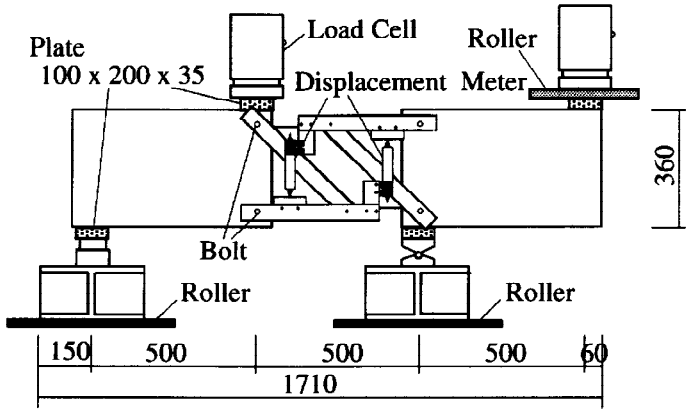

Fig. 2 Loading and measuring apparatus (unit: mm)

The compressive strength of concrete was 19.5 MPa. The yield strengths of the main bars, D22 and D13, were as high as 932 and 1044 MPa to prevent flexural failure. The yield strengths of shear reinforcement, S6 and S8, were also as high as 896 and 995 MPa to enhance three dimensional shear failure, as will be discussed later.

The relationships observed between shear force and deflection are shown in Fig. 4. At their maximum deflections, fluorescent epoxy resin was injected into the specimens. After the tests, the specimens were sawed in transverse directions at the section indicated by the broken line in Fig. 2(b). Examples of the photos of the sawed sections are shown in Fig. 5, where most of the cracks are curved, which means that shear failure was three dimensional.

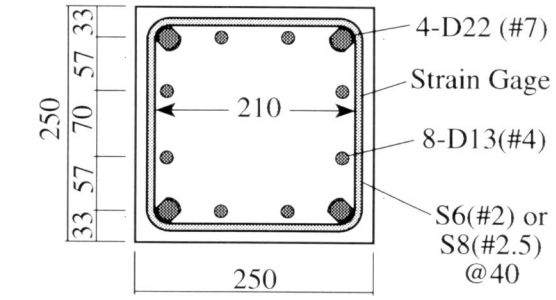

(a) Section

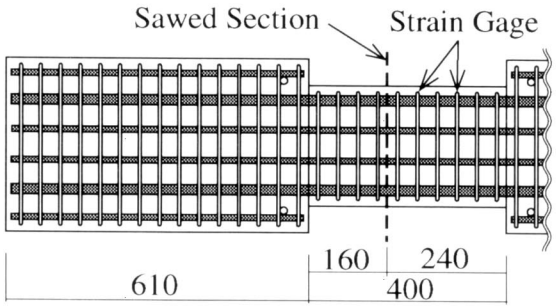

(b) Side View

Fig. 3 Specimens Detail (unit: mm)

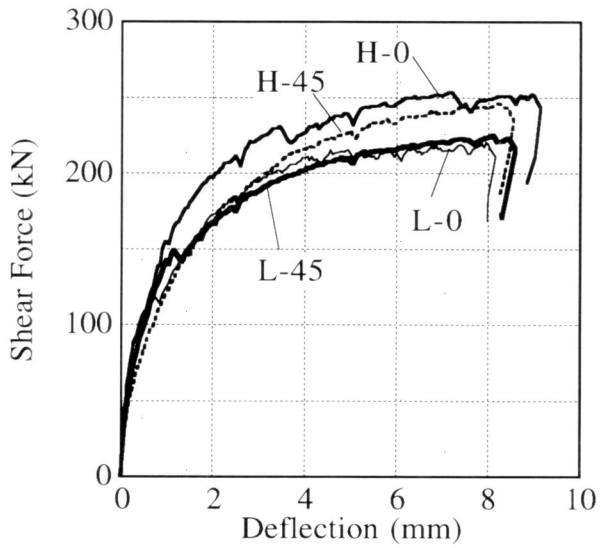

Fig. 4 Shear force vs. deflection relationships

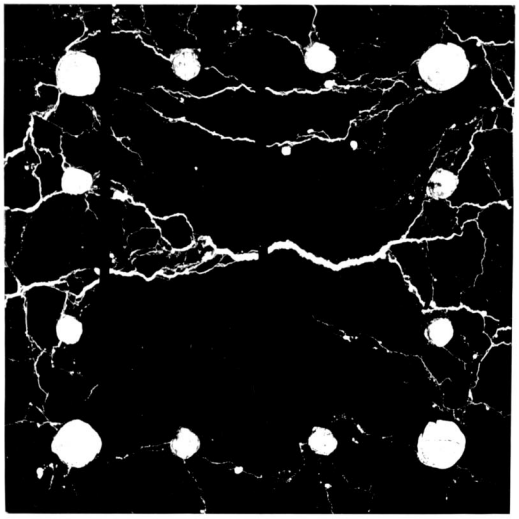

(a) Specimen L-0

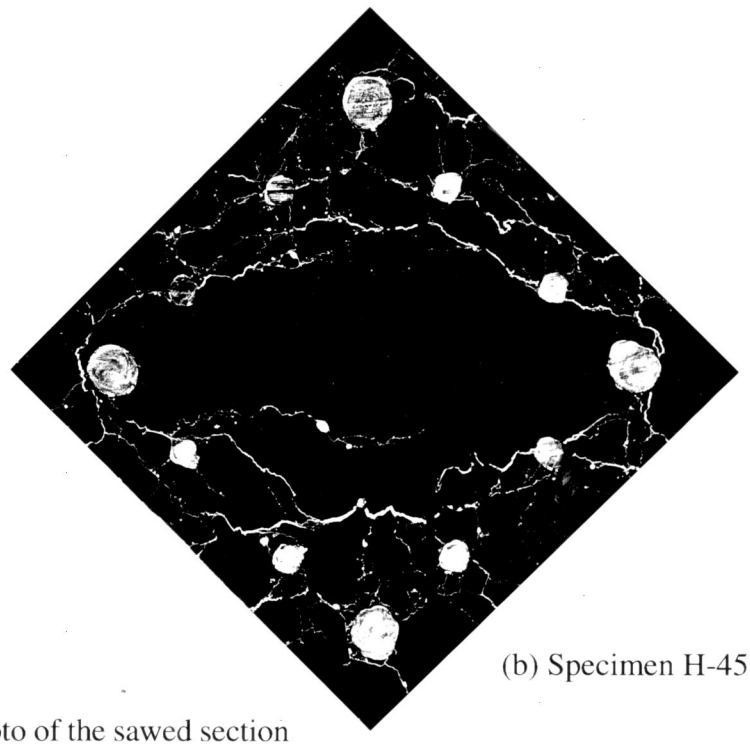

(b) Specimen H-45

Fig. 5 Photo of the sawed section

PLASTICITY ANALYSIS BASED ON THE UPPER BOUND THEOREM

Assumptions

1) Longitudinal reinforcement is sufficiently strong and rigid in the longitudinal direction.
2) Dowel action of longitudinal reinforcement is sufficiently small.
3) Shear reinforcement is rigid-plastic.
4) Concrete is rigid-plastic having a yield locus as shown in Fig. 6, where σ_e is effective strength calculated as follows. (See Ichinose *et al.*, [1992] for derivation.)

$$\sigma_B < 20 \text{ MPa} \quad \sigma_e = 0.85\,\sigma_B \tag{2}$$

$$\sigma_B \geq 20 \text{ MPa} \quad \sigma_e = 0.4\,\sigma_B + 9 \text{ (MPa)} \tag{3}$$

where σ_B is compressive strength of concrete. Tensile strength of concrete is negligible.

5) Concrete is effective inside the shaded region in Fig. 7, which is confined by the outer stirrup.
6) Concrete fails at planes explained in the following section.

Failure Planes

Since the longitudinal reinforcement is sufficiently strong and rigid, the relative displacement occurs vertically as shown in Fig. 8. The work equation is as follows:

$$W_e = W_C + W_S \tag{4}$$

where $W_e = V.u$ is the external work defined as the product of the shear force V and a virtual deflection u; W_C

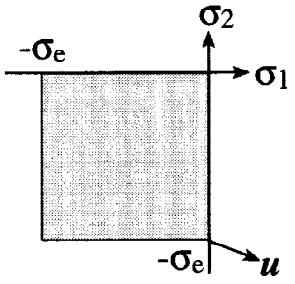

Fig. 6 Yield Locus of Concrete

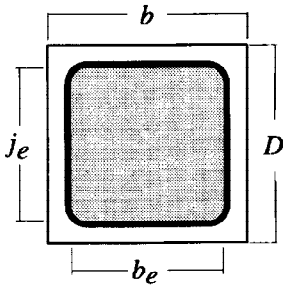

Fig. 7 Effective Section

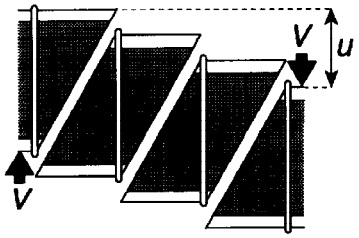

Fig. 8 Relative Displacement

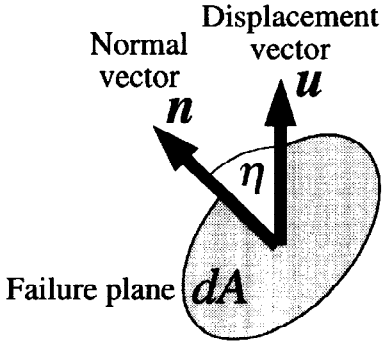

Fig. 9 Minimal Failure Plane

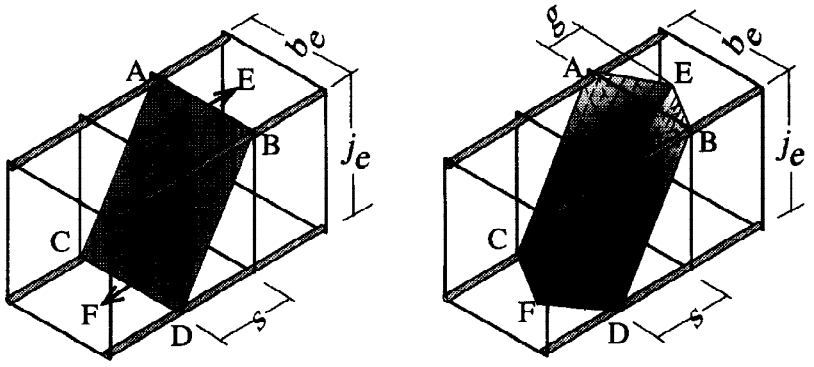

(a) Flat Plane (b) Curved Plane

Fig. 10 Shear Failure Planes in 0 Degree

and W_S are the internal work done by concrete and shear reinforcement, respectively. The shear strength is obtained dividing $W_C + W_S$ by u.

The internal work done in the minimal failure plane, dA in Fig. 9, is as follows [see Nielsen (1984) for derivation]:

$$dW_c = \frac{(1-\cos\eta_i)\sigma_e dA}{2} u \tag{5}$$

where η is the angle between the displacement vector $\boldsymbol{u}$ and the normal vector $\boldsymbol{n}$. Integrating this over the whole failure plane, we have W_C.

$$W_c = \int dW_c \tag{6}$$

In such analysis, shear failure has normally been assumed to occur in flat planes shown in Fig. 10(a). However, shear failure may be assumed to occur in curved planes shown in Fig. 10(b), a ruled surface made of a set of segments moving from AC to BD through EF, which makes W_C smaller than the flat plane. Figure 11 shows the relationship between W_C and the depth of the valley, g in Fig. 10(b) for the case that $s = 0.6j_e$, where W_C is normalized by W_{CO}, the inner work done by the flat plane of Fig. 10(a). The depth of the valley, g, is determined to minimize W_C.

The works done by the shear reinforcement between AB and E is negligible, since the reinforcement is deformed like Fig. 12 yielding only flexural deformation, which resistance is negligible. In other words, the depth of the valley, g, does not affect W_S in Eq. 4. Thus, the curved plane in Fig. 10(b) makes smaller W_e than the flat plane. According to the upper bound theorem, the curved plane is more probable than the flat plane.

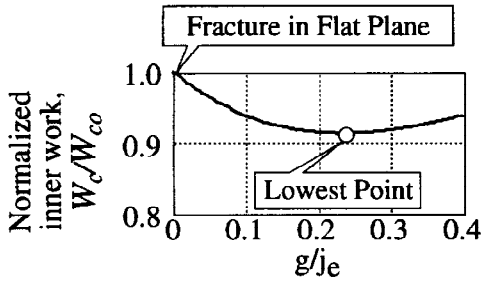

Fig. 11 Inner work of concrete affected by the depth of the valley, g

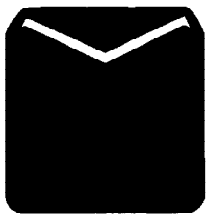

Fig. 12 Flexural Deformation of Shear Reinforcement

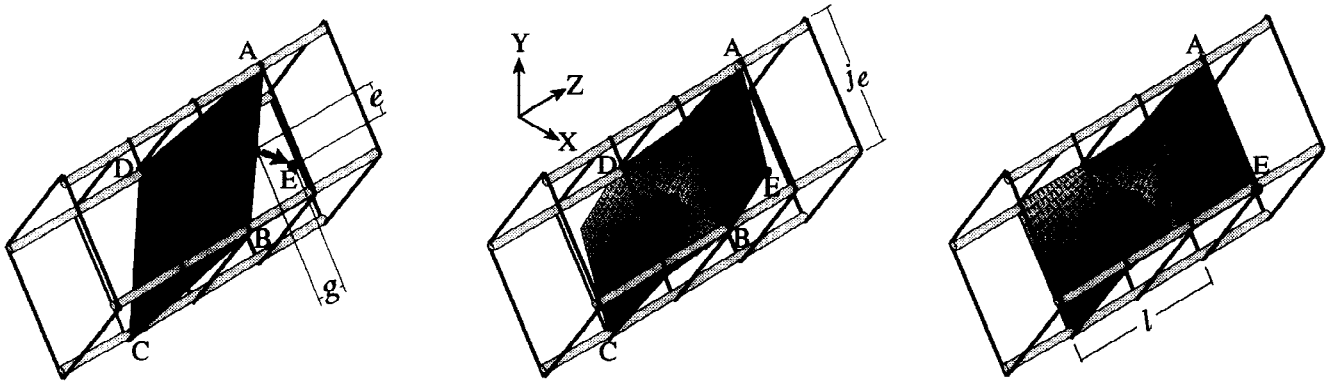

(a) Flat Plane (b) Curved Plane (Assumed) (c) Curved Plane (Calculated)

Fig. 13 Shear Failure Planes in 45 Degree

Similarly, the curved plane shown in Fig. 13(b), a ruled surface made of a set of segments moving from BE to OA, is more probable than the flat plane in Fig. 13(a) for 45 degree loading. The movement of the point E, g and e of Fig. 13(b), is again determined to minimize W_C. In all the cases, the point E moved to the edge of the specimen as shown in Fig. 13(c).

Result 1 -- Effect of Loading Direction

Shear force V increases as tensile stress in shear reinforcement σ_w increases. Using the method shown above, the shear strengths of the tested specimens are calculated assuming various tensile stress in the shear reinforcement, and the results are normalized and shown in Fig. 14. The observed relationships between the shear force and the stress in the shear reinforcement are also shown in Fig. 14. They agree well.

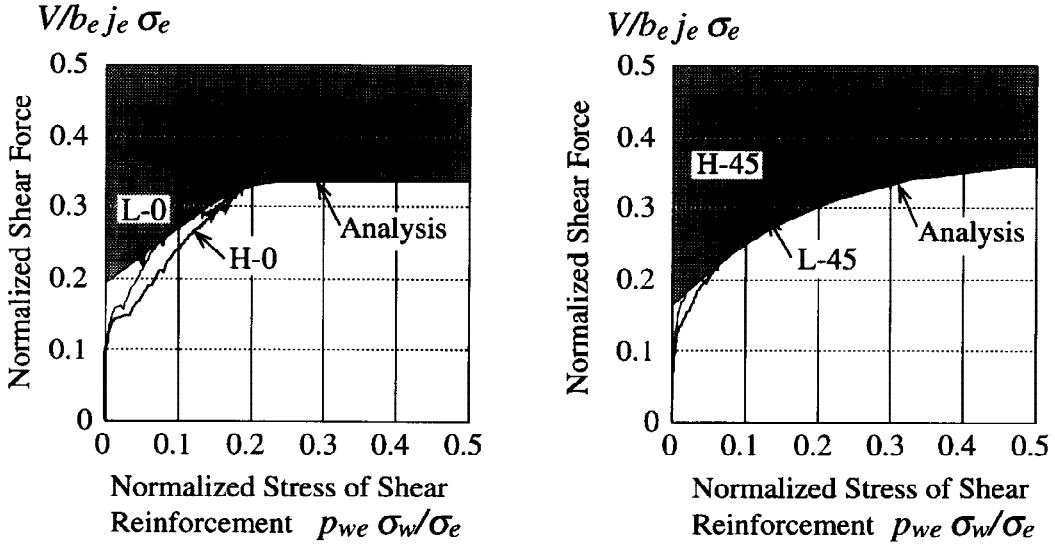

(a) 0 degree loading (b) 45 degree loading

Fig. 14 Shear Force vs. Stirrup Stress

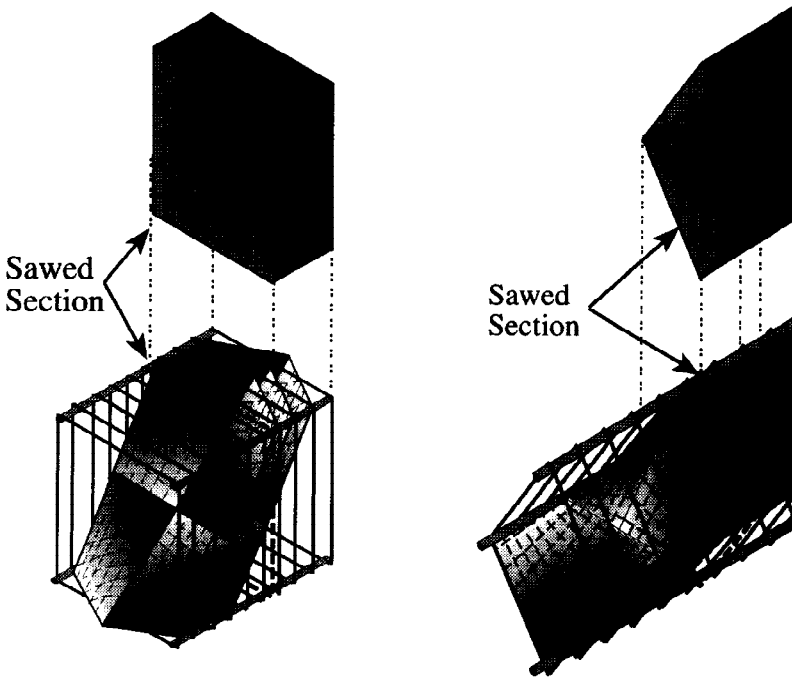

(a) 0 degree loading (b) 45 degree loading

Fig. 15 Calculated Failure Planes

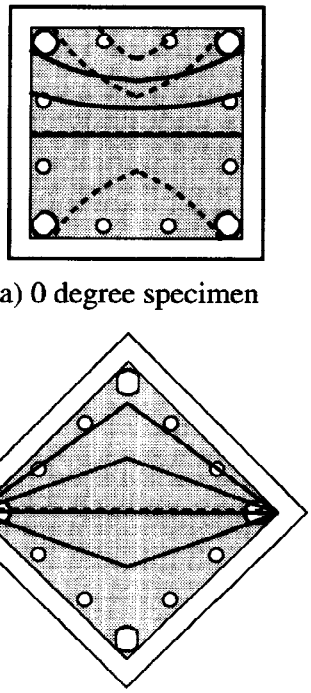

(a) 0 degree specimen

(b) 45 degree specimen

Fig. 16 Sawed Section

A specimen may have several failure planes at the same time as shown in Fig. 15. The solid and broken lines in Fig. 16 indicate the calculated failure planes in the sawed sections when the specimens are at their calculated strengths and 95% of them, respectively. In the 0 degree specimens, the failure planes are curved inward; whereas in the 45 degree specimens, the failure planes are curved outward. These tendencies agree with the observation in Fig. 5.

Result 2 -- Effect of Sub-ties

A section with sub-ties cannot be curved as in Fig. 10(b), since it elongates the shear reinforcement between AB and E, making the internal work by shear reinforcement W_e larger. Instead, the failure plane may be curved only between the sub-ties as shown in Fig. 17. Thus, the failure plane becomes flatter if sub-ties exist in the section.

The specimens of Ichinose *et al.* (1995), In50 and Out50, are analyzed to examine the effect of sub-ties. They had identical properties including shear reinforcement ratio (1.7%) except that In50 had sub-ties and Out50 did not, as shown in Fig. 18. The observed cracks of the specimens In50 (with sub-ties) and Out50 (without

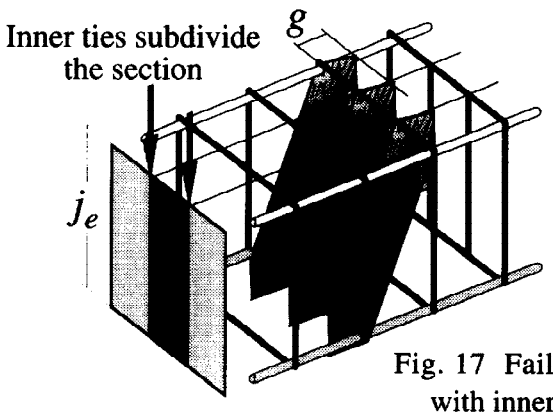

Fig. 17 Failure plane with inner ties

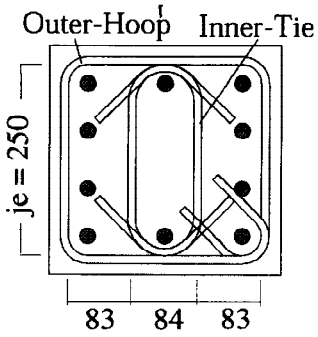

(a) Specimen In50

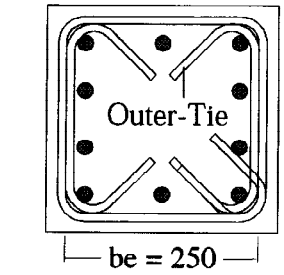

(b) Specimen Out50

Fig. 18 Specimen Section

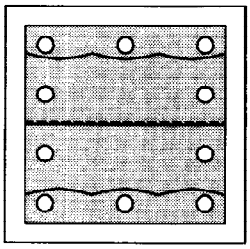

(a) Specimen In50

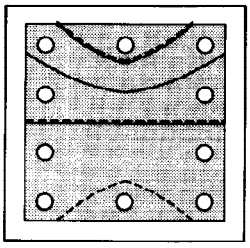

(b) Specimen Out50

Fig. 19 Calculated Failure

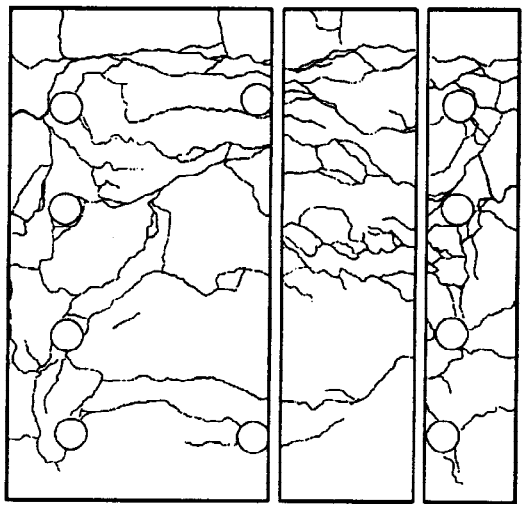

(a) Specimen In50

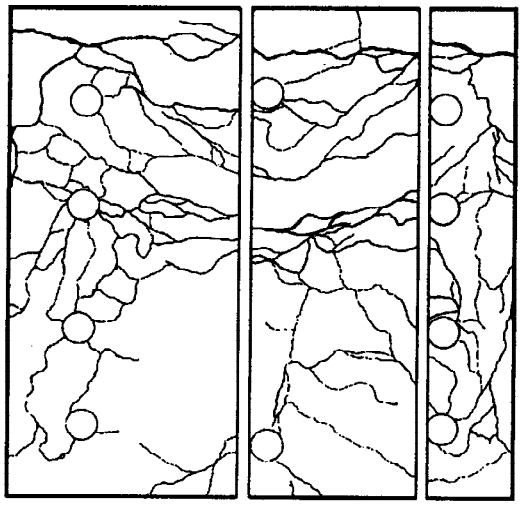

(b) Specimen Out50

Fig. 20 Cracks at the Sawed Section

sub-ties) are shown in Fig. 20. The solid and broken lines in Fig. 19 indicate the calculated failure planes in the sawed sections when the specimens are at their strengths and 95% of them, respectively. Figure 20 is similar to Fig. 19.

The shear strengths of the specimens are calculated assuming various tensile stress in the shear reinforcement, and the results are shown in Fig. 21. The observed relationships between the shear force and the stress in the shear reinforcement are also shown in Fig. 21. They agree well.

CONCLUSIONS

Three dimensional shear failure was observed in reinforced concrete columns subjected to shear in 0 and 45 degree. Analyses based on the upper bound theorem of plasticity explained the failure as well as the effects of sub-ties on shear strengths of columns.

REFERENCES

Ichinose, T. and K. Hanya, (1995). Three dimensional shear failure of RC columns, *Concrete under severe conditions: Environment and loading*, Vol. 2, E & FN Spon, pp. 1737-1747

Ichinose, T. and S. Yokoo, (1992). Shear strength of R/C beams with spiral reinforcement, *J. of Struct. and Constr. Engng*, Architectural Institute of Japan, No. 441, pp. 85-91 (in Japanese)

Nielsen, M. P. (1984). *Limit analysis and concrete plasticity*, Prentice Hall, USA.

Schlaich, J., Schaefer, K. and Jennewein, M. (1987). Toward a consistent design of structural concrete, *PCI Journal*, pp. 74-150

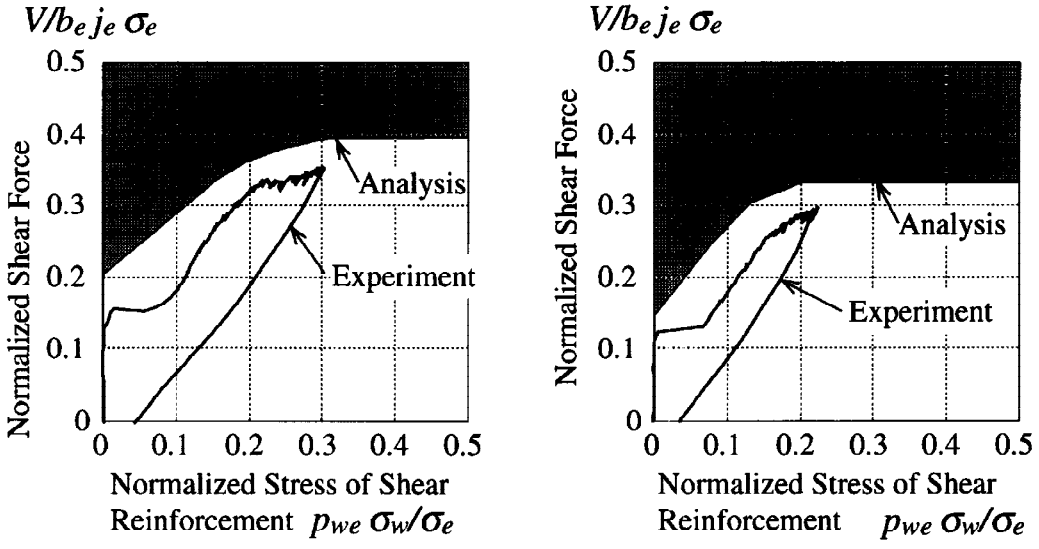

(a) Specimen In50 (b) Specimen Out50

Fig. 21 Shear Force vs. Stirrup Stress